Acta Radiologica Open
5(9) 1–11

DOI: 10.1177/2058460116668216
arr.sagepub.com

Whole-body MRI for full assessment and characterization of diffuse inflammatory myopathy

Saleh Saleh Elessawy[1], Eman Muhammad Abdelsalam[1], Eman Abdel Razek[2] and Samar Tharwat[3]

Abstract

Background: Conventional magnetic resonance imaging (MRI) is a highly valuable tool for full assessment of the extent of bilateral symmetrical diffuse inflammatory myopathy, owing to its high sensitivity in the detection of edema which correlates with, and sometimes precedes, clinical findings.

Purpose: To evaluate the use of whole-body (WB)-MRI in characterization and full assessment of the extent and distribution of diffuse inflammatory myopathy.

Material and Methods: A prospective study on 15 patients presenting with clinical evidence of inflammatory myopathy. It included 4 boys/men and 11 girls/women (age range, 6–44 years; mean age, 25.5 years). 1.5 T WB-MRI was performed and the distribution and extent of disease severity was assessed according to muscle edema on STIR images.

Results: Four cases of dermatomyositis showed lower limb disease predilection with edema in gluteal, thigh, and calf muscles. The same finding was seen in one case with recurrent polymyositis and three cases with overlap myositis with systemic lupus erythematosus (SLE). Bilateral upper and lower limb myositis was demonstrated in three cases of polymyositis and one case of overlap myositis with scleroderma. Bilateral edema involving all scanned muscle groups was detected in three cases of polymyositis with paraneoplastic syndrome, SLE, and severe active dermatomyositis (including the neck muscles).

Conclusion: WB-MRI is the diagnostic modality of choice for cases of inflammatory myopathy. It accurately detects the most severely affected muscles candidate for biopsy and provides a reliable baseline study for follow-up of disease progression as well as response to treatment.

Keywords
Polymyositis, dermatomyositis, magnetic resonance imaging (MRI), whole body MRI, systemic lupus erythematosus

Date received: 13 April 2016; accepted: 15 August 2016

Introduction

Inflammatory myopathies represent a heterogeneous group of acquired disorders, all of which feature symmetric proximal muscle weakness, increased serum levels of muscle derived enzymes, and non-suppurative inflammation of skeletal muscle (1).

The most common idiopathic myositis is dermatomyositis (DM); the disease onset is in childhood, hence the term juvenile dermatomyositis, and is more common in girls than boys (2). The second most common is polymyositis (PM), which is an idiopathic autoimmune myopathy sparing the skin with a later

[1]Radiodiagnosis Department, Mansoura Faculty of Medicine, Mansoura University, Mansoura, Egypt
[2]Physical Medicine, Rheumatology and Rehabilitation Department, Mansoura Faculty of Medicine, Mansoura University, Mansoura, Egypt
[3]Internal Medicine Department, Rheumatology and Immunology Unit, Mansoura Faculty of Medicine, Mansoura University, Mansoura, Egypt

Corresponding author:
Eman Muhammad Abdelsalam, Radiolodiagnosis Department, Faculty of Medicine, Mansoura University, Mansoura, Egypt.
Email: emanmohamad.em@gmail.com

onset than DM. It may occur as a part of paraneoplastic syndrome and manifest long before the underlying malignancy is recognized (3).

The least common type is inclusion body myositis (IBM). It is characterized by gradual onset and may take several months from the onset of symptoms till the diagnosis is made and this time can be as long as 6 years. IBM may be associated with other connective tissue diseases in about 15% of patients (4).

A diagnostic dilemma occurs when autoimmune myositis overlaps a pre-existing connective tissue disease. In such cases, for definitive diagnosis, muscle biopsy is required. Unfortunately, muscle biopsy is a painful procedure associated with significant morbidity when repeated (5).

The essential role of conventional magnetic resonance imaging (MRI) in the detection and assessment of the extent of bilateral myopathy has been established in the literature (6–9). Moreover, muscle biopsy yields successful results after selection of the most severely affected muscle based on MRI findings (10).

A limitation of conventional MRI has been an inability to scan a large volume of muscles without prolonged acquisition times. In general, only symptomatic muscles are imaged. Whole-body MRI (WB-MRI) has the advantage of documenting inflammatory myopathy of multiple muscle groups, including the psoas, intercostal, and neck muscles, not imaged using standard protocols. In addition, the distal upper and lower limb muscles can be imaged with little extra scanning time (3).

WB-MRI allows true whole-body scanning with broad analysis of muscle involvement by contiguous axial sections extending from head to toe and coronal sections from the anterior to the posterior surface of the body (11). The aims were to attempt to evaluate the use of WB-MRI in characterization and full assessment of the extent and distribution of diffuse myositis due to idiopathic myopathies as well as autoimmune disease overlap.

Material and Methods

Patients

This prospective research study was carried out in the radiology department on cases referred to the MRI unit for whole-body scanning from the rheumatology and immunology departments in the period between April 2014 and November 2015. Acceptance from the Research Institutional Board was granted (code number: R/16.02.05) and informed consent was waived from adult patients and children's parents for performing WB-MRI and US-guided muscle biopsy for genetic analysis.

The study included 4 boys/men and 11 girls/women (age range, 6–44 years; mean age, 25.5 years). WB-MRI was also conducted on five male and five female age-matched controls. Clinical diagnosis of five cases of dermatomyositis was based on the Bohan and Peter criteria for dermatomyositis (12): ''muscle weakness, positive muscle biopsy, elevated serum enzyme levels, positive EMG and characteristic rash of DM. Definite PM = all 4, probable PM = 3 of 4, possible PM = 2 of 4; Definite DM = rash + 3 other; probable DM = rash + 2 other; possible DM = rash + 1 other.''

Patients with polymyositis (four cases) had symptoms of bilateral proximal limb weakness, with additional calf discomfort in two out of four cases. Five patients had a history of underlying connective tissue disease (four with systemic lupus erythematosus [SLE] and one with scleroderma). One case presented with bilateral proximal upper and lower limb weakness, with a history of surgery for high grade glioma and was diagnosed as myositis due to paraneoplastic syndrome.

Inclusion criteria: patients presenting with clinical evidence of inflammatory myopathy; duration $\leq$3 years, based on bilateral symmetric proximal limb weakness, raised serum skeletal muscle enzymes (CK >215 IU/L; normal range, 20–215 IU/L) and electromyography (EMG) results (Tables 1–3). Exclusion criteria: muscular dystrophy, metabolic or endocrine myopathy, toxic myopathy, granulomatous and infectious myositis.

All patients underwent the evaluation of muscle disease activity using the myositis disease activity assessment tool:

Myositis disease activity assessment tool, Version 2 – 2005:
This is a combined tool that includes:
(i) Myositis disease activity assessment visual analogue scales (MYOACT).
(ii) Myositis intention to treat activity index (MITAX).

Myositis intention to treat activity index (MITAX)
This scoring system is composed of six individual organ systems (constitutional, cutaneous, skeletal, gastrointestinal, pulmonary, and cardiac). Each system is scored by using a 10 cm visual analogue scale (VAS) by drawing a vertical mark on the 10 cm and a line for each system is is drawn according to the following scale: left end of the line, no evidence of disease activity; mid-point of the line, moderate disease activity; and right end of the line, extreme or maximum disease activity. Then, the total score is the sum of the scores for each one and divided by the total possible score (range, 0–60) (13).

In case one or more system is not evaluated, the resulting score would be divided by the maximum

Table 1. Laboratory investigation and manual muscle testing.

Cases	Sex	Serum CK (IU/L)	Serum aldolase	Manual muscle testing
Dermatomyositis	Female	235	11	8–9/10
Dermatomyositis	Female	798	15	6–7/10
Dermatomyositis	Male	4500	20	2–3/10
Overlap myositis (SLE)	Female	560	17	6–7/10
Polymyositis	Male	2100	20	3–4/10
Dermatomyositis	Female	452	14	
Overlap myositis (Scleroderma)	Female	250	11	4–5/10
Overlap myositis (SLE)	Female	289	13	7–8/10
Polymyositis	Male	5430	24	7–8/10
Overlap myositis (SLE)	Male	2500	20	2–3/10
Polymyositis	Male	178	5	2–3/10
Dermatomyositis	Female	3600	22	10/10
Polymyositis	Male	99	3	2–3/10
Paraneoplastic syndrome	Female	3200	21	9/10
Overlap myositis (SLE)	Female	6300	27	2–3/10

possible score from those assessed items. The categories of other disease activity, global extra-skeletal muscle, muscle and global disease activity are not included in the MYOACT score but are scored separately. In our study, VAS was requested from all the patients and the assessment included only four systems (constitutional, skeletal, cutaneous, and muscle disease activity). The category muscle disease activity was evaluated separately.

Myositis intention to treat activity index (MITAX)

The recording is based upon the following criteria (14): (i) the presence of clinical features at this time or within the previous 4 weeks; (ii) the clinical feature is due to myositis for each item of the MITAX. The scoring system is based on the physician's intention to treat categories (range, A–E): A, if the feature is thought to be sufficiently active to require disease modifying treatment (9 points); B, if the feature is less active than A—moderate activity requiring moderate therapies (3 points); C, if the feature is stable or mild, requiring only symptomatic therapy (1 point); D, if the feature has resolved (no medication is required) (0 points); E, if the feature has never been present; and NA, if the feature cannot be assessed.

If more than one clinical symptom is present within a system, and different categories would be scored for each, the scoring is based upon the category that is most severe. This scoring system is composed of seven individual organ systems (constitutional, cutaneous, skeletal, gastrointestinal, pulmonary, and cardiac); the total score is the sum of the scores for each one and divided by the total possible score (range, 1–63).

Muscle power was determined using manual muscle testing 8 (15) as a helpful tool to assess the muscle disease activity. In addition, electromyographic studies (EMG) were done for all the patients and showed findings suggestive for myopathy, including: increased insertional activity, positive sharp wave and fibrillation during spontaneous activity. During normal volition: increased polyphasicity, decreased amplitude and short duration of motor unit action potential was reported. During maximal volition: complete interference pattern was recorded, but with decreased amplitude and short duration. These findings were present in all clinically active cases while EMG findings were normal in clinically inactive and controlled cases. A past history of positive EMG findings in all patients was a helpful tool for the diagnosis and completed the diagnostic criteria of the inflammatory myositis.

Imaging

All images were acquired using a 1.5 T MR scanner (Achieva; Philips Medical Systems, Best, The Netherlands). Imaging was performed in the coronal plane using turbo T1 and STIR sequences. Excitation and signal acquisition were acquired using body coil. Initial scanning with sagittal and coronal views was performed for localization.

The following pulse sequences were used: coronal Turbo STIR images (TR, 3000–4000 ms, TE, 60 ms, TI, 140 ms; field of view (FOV), 200–500 mm; matrix, 128–140 × 256). Coronal T1-weighted images were acquired using: TR, 600 ms; TE, 15 ms; FOV, 200–500 mm; matrix, 150–180 × 256. Additional T1 (TR, 698 ms; TE, 15 ms) and STIR (TR, 3000–3500 ms; TE, 60 ms; TI, 140 ms) images were obtained in the axial view when required for better assessment. Acquisition time was 15–20 min. None of the cases was given contrast medium, as all cases presented with diffuse inflammatory process, no masses, abscesses, or mass-like lesions.

For whole-body coverage, coronal slabs were constructed at contiguous (4–6) stations. Slice thickness was 8 mm with an interslice gap of 0.8 mm. The number of coronal slices varied according to the patient's stature. Respiratory triggering was used. The generated WB-MR images were reviewed by the interpreting radiologist with 8 years of experience (second author) with a PhD and musculo-skeletal subspecialty for 3 years. This was under the supervision of a specialized professor in Musculoskeletal Radiology.

Table 2. Myositis disease activity assessment.

Cases	VAS for muscle disease activity	VAS for constitutional: pyrexia, fatigue, weight loss	VAS for cutaneous disease activity	VAS for skeletal disease activity	Total score of the MYOACT
Dermatomyositis	3	3	2	0	0.16
Dermatomyositis	5	5	0	0	0.16
Dermatomyositis	10	7	5	6	0.6
Overlap myositis (SLE)	5	5	5	2	0.4
Polymyositis	8	6	5	5	0.53
Dermatomyositis	5	5	5	1	0.36
Overlap myositis (Scleroderma)	3	2	0	0	0.06
Overlap myositis (SLE)	4	2	2	1	0.16
Polymyositis	10	8	0	7	0.5
Overlap myositis (SLE)	8	7	7	5	0.63
Polymyositis	0	0	0	0	0
Dermatomyositis	9	8	5	6	0.63
Polymyositis	0	0	0	0	0
Paraneoplastic syndrome	9	7	0	0	0.23
Overlap myositis (SLE)	10	10	5	8	0.76

MYOACT, myositis disease activity assessment visual analog scales; VAS, Visual Analog Score.

Table 3. Myositis intention to treat activity index (MITAX).

Cases	Muscle disease activity (MITAX)	Constitutional (MITAX)	Cutaneous disease activity (MITAX)	Skeletal muscle disease activity (MITAX)	Total score of (MITAX)
Dermatomyositis	C	C	C	D	0.07
Dermatomyositis	B	B	D	D	0.11
Dermatomyositis	A	A	B	A	0.22
Overlap myositis (SLE)	B	B	B	C	0.22
Polymyositis	A	A	B	B	0.55
Dermatomyositis	B	B	B	C	0.22
Overlap myositis (scleroderma)	C	C	D	E	0.03
Overlap myositis (SLE)	C	C	C	C	0.11
Polymyositis	A	A	E	A	0.66
Overlap myositis (SLE)	A	A	A	B	0.77
Polymyositis	D	D	D	D	0
Dermatomyositis	A	A	B	A	0.77
Polymyositis	D	D	E	D	0
Paraneoplastic syndrome	A	A	E	E	0.33
Overlap myositis (SLE)	A	A	B	A	0.77

A, highly active and need disease modifying treatment = 9 points; B, moderate activity requiring moderate therapies = 3 points; C, mild activity and requiring symptomatic therapy = 0 points; D, resolved (no medication is required) = 0 points; E, has never been present; NA, cannot be assessed.

MRI evaluation

Disease distribution:

- Muscle affection: muscles of the neck, shoulder girdle, thorax, abdomen, pelvis, thighs, and legs in the calf region were assessed for symmetric or asymmetric distribution of diffuse edema and/or fatty infiltration, diffuse muscle atrophy, or swelling.
- Joint affection: effusion, degenerative changes, avascular necrosis.
- Soft tissue affection: subcutaneous edema, intermuscular and perimuscular fascial edema, skin and subcutaneous nodules.
- Disease extent: by semi-quantitative analysis, grading was according to the protocol described by Quijano-Roy et al. (11). STIR sequence was performed for assessment of edema and abnormal intramuscular bright signal was scored as: 1, subtle intramuscular hyperintensity; 2, easily detectable intramuscular hyperintensity; and 3, intense intramuscular hyperintensity.

Statistical analysis

Statistical analysis was done using statistical package (SPSS, Version 20 for Windows, SPSS Inc., Chicago, IL, USA). Demographic variables were summarized as medians and ranges for non-normally distributed continuous variables and as frequencies for categorical variables. Pearson's correlation coefficient was used for correlation between MRI grading of edema and disease severity on clinical assessment.

Results

Clinical evaluation and muscle disease activity scores are summarized in Tables 1–3.

WB-MRI findings are summarized in Table 4.

WB-MR images of the control group of age-matched healthy individuals were regarded as a baseline study for normal appearance of muscles on T1 and STIR sequences; with no detectable edema or fatty infiltration.

In four cases of dermatomyositis, WB-MRI revealed grade 1 (2/5), grade 2 (1/5), and grade 3 (1/5) lower limb disease predilection in the form of edema in the gluteal, thigh, and calf muscles. The same finding was seen in one case with recurrent polymyositis (grade 1) and three cases with overlap myositis with SLE (grade 1, 2/4; grade 2, 1/4). Bilateral upper and lower limb predilection was demonstrated in three cases of polymyositis (grade 1, 2/4; grade 2, 1/4) and one case of overlap myositis with scleroderma (Table 4).

Subcutaneous edema and fascial edema was a common finding seen in moderately to markedly affected cases of inflammatory myopathy (Figs. 1–3). Skin nodules could also be detected in dermatomyositis (Fig. 1b and c).

Severe bilateral muscle edema (grade 3) involving all scanned muscle groups was detected in two cases of polymyositis with paraneoplastic syndrome and SLE and one case of severe active dermatomyositis (including the neck muscles).

Muscle selection for biopsy was based on the MRI appearance; in which biopsy was taken from the most severely affected muscle with the highest grade of edema. As an example, MRI ruled out the necessity for repeated biopsy in a 13-year-old boy diagnosed with polymyositis. He presented with constitutional manifestations in the form of bilateral muscle weakness. Yet, laboratory studies and clinical evaluation were within the normal range. WB-MRI was requested and the only finding was subtle bilateral edema in antero-lateral thigh muscles. Consequently, the patient received symptomatic treatment instead of immune-suppressive therapy.

Moreover, significant statistical correlation was found between the grade of muscle edema estimated by MRI and the clinical assessment through VAS for muscle disease activity ($r = 0.9$) as well as Myositis Intention to Treat Activity Index (MITAX) grading of muscle disease activity ($r = 0.8$).

Discussion

Conventional MRI was used to provide highly valuable findings to confirm the diagnosis of idiopathic inflammatory myopathy (16–18). However, the confinement to the symptomatic limbs may result in missing early myositis in asymptomatic muscles (3). That is why WB-MRI is useful to fully address the disease burden without the need for multiple painful biopsies or electromyograms.

In our study we attempted to assess the role of WB-MRI in the diagnosis of diffuse myositis in a variety of cases referred from rheumatology and immunology departments throughout the period of investigation. WB-MRI allows for the visualization of all muscles of the body with few exceptions such as the diaphragm, oculomotor, and facial muscles (11). With this modality we analyzed initial and recurrent cases of dermatomyositis and polymyositis regarding extent and distribution of muscle, fascia, skin, and subcutaneous fat affection.

Bilateral symmetrical diffuse muscle edema was the hallmark of diagnosis for all cases included in the study. The role of MRI was to detect the distribution of edema (which reflects the inflammatory process

Table 4. Distribution and grades of edema.

	Distribution							Grade		
Disease	Neck	Upper limb	Thorax	Abdomen	Pelvic girdle	Thighs	Calf region	I Mild	II Moderate	III Marked
Dermat-myositis (5 cases)	Multifidus, semi-spinalis cervicus, semi-spinalis capitis, sternocleiomastoid (n = 1)	Shoulder, arm and forearm: deltoid, subscapularis, supraspinatus, infraspinatus: teres major, triceps, biceps, brachialis, coracobrachialis (n = 1)	Trapezius, latissimus dorsi, erector spinae, scalene and intercostal muscles (n = 1)	Erector spinae, psoas muscles (n = 1)	Iliopsoas, sartorius, rectus femoris, obturator muscles, pectineus (n = 1); gluteal muscles (n = 3)	Vastus lateralis (n = 5); vastus intermedius (n = 3); adductor magnus (n = 5); hamstring (n = 2)	Medial and lateral head of gastrocnemius (n = 5); soleus (n = 5); peroneal and tibialis anterior and posterior muscles (n = 1)	2	1	2
Poly-myositis (4 cases)	–	Shoulder and upper arm subscapularis, supraspinatus (n = 2); infraspinatus, teres major, deltoid, triceps (n = 1)	Erector spinae, intercostal (n = 2); trapezius, latissimus dorsi (n = 1)	Erector spinae, psoas muscles (n = 1)	Iliopsoas, sartorius, rectus femoris, obturators, pectineus (n = 1); gluteal muscles (n = 4)	Vastus lateralis and vastus intermedius (n = 2); adductor magnus (n = 2)	Medial and lateral head of gastrocnemius (n = 2); soleus (n = 1)	2	0	2
Paraneoplastic syndrome (1 case)	–	Subscapularis, supraspinatus, infraspinatus, teres major, deltoid coracobrachialis	–	–	Iliopsoas, sartorius, rectus femoris, obturators, pectineus and gluteal muscles	Vastus lateralis, vastus intermedius, adductor magnus, hamstring muscles	Medial and lateral head of gastrocnemius, soleus, peroneal and tibialis anterior and posterior muscles and all muscles of distal legs are affected down to the sole of the foot			1
SLE (4 cases)	–	Shoulder and upper arm, subscapularis, supraspinatus, infraspinatus, teres major, deltoid, triceps, coracobrachialis (n = 1)	Trapezius, latissimus dorsi, erector spinae (n = 1)	Erector spinae, psoas muscles (n = 1)	Iliopsoas, sartorius, rectus femoris, obturators, pectineus (n = 2); gluteal muscles (n = 4)	Vastus lateralis and vastus intermedius (n = 4); adductor magnus (n = 2); hamstring (n = 2)	Medial and lateral head of gastrocnemius, soleus, peroneal and tibialis anterior and posterior muscles (n = 1)	2	1	1
Scleroderma (1 case)	–	Shoulder and upper arm subscapularis, supraspinatus, infraspinatus, teres major, deltoid, triceps	Erector spinae, latissimus dorsi	–	Gluteal muscles	Vastus lateralis			1	

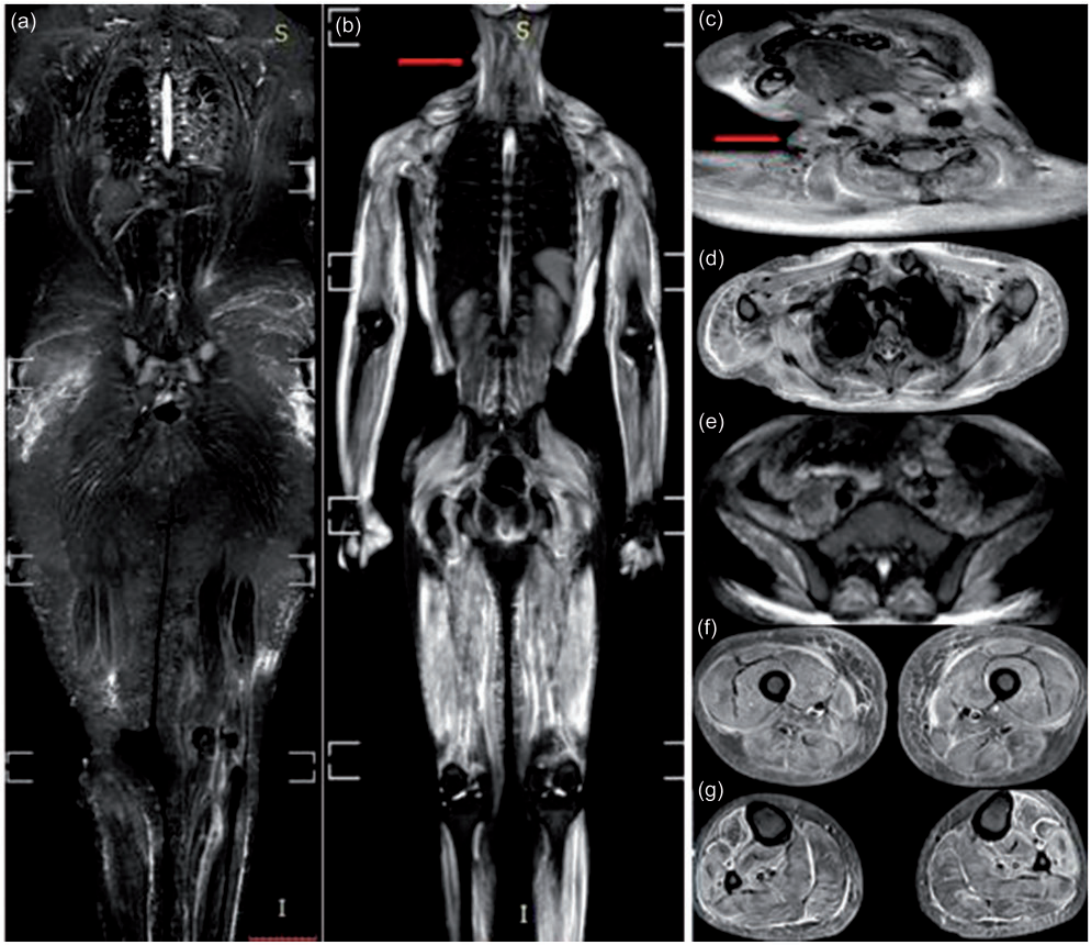

Fig. 1. WB-MRI, STIR sequence for two cases of dermatomyositis. (a) Case 1: mild bilateral symmetrical edema of the gluteal, thigh, and calf muscles with interstitial edema of the subcutaneous fat of the gluteal region and thighs. Case 2: (b) marked bilateral symmetrical edema of all muscle groups: neck (c), the shoulder girdle and thoracic wall (d), the pelvic girdle (e), the thigh (f), and calf (g) muscles. Marked interstitial edema is clearly evident in the upper arms and the lateral aspect of the chest wall. Note: a skin nodule is seen on the right lateral aspect of the neck (arrow in b, c).

involving the affected muscles) and the extent of muscle affection by grading the severity of edema.

From our results we can deduce that in cases with idiopathic inflammatory myopathy, initial disease predilection is for the lower limb muscles: the pelvic, gluteal, and thigh muscles, particularly the gluteus maximus, vastus lateralis, and vastus intermedius. The adductor magnus and hamstring muscles are less commonly affected. This is followed by progressive involvement of the shoulder girdle and the thoracic and neck muscles (Table 4). This classic bilateral disease predilection is in agreement with previous studies (3,19,20).

An important remark is the affection of calf muscles; medial and lateral heads of gastrocnemius and soleus are the most common, yet, in cases of severe acute myositis, significant affection of all calf muscles including tibialis anterior, peroneus longus, and breves, together with muscle swelling was clearly evident in severely affected cases (Figs. 1g and 2b). That is why we draw the attention towards including proximal leg muscle involvement as part of the diagnostic checklist in bilateral lower limb conventional MRI or WB-MRI.

Furthermore, we relied on coronal T1 WB-MRI for detection of subcutaneous interstitial edema (Fig. 3g and h) which is presumed to be as a result of perivascular inflammation (21). It was detected in severely affected cases rather than mildly affected ones; this finding is in agreement with Ladd et al. (20). However, the distribution of subcutaneous edema did not mirror the distribution of skin rash in cases of dermatomyositis; this finding is discordant with that reported by Ryan et al. (19).

Severe polymyositis as a part of paraneoplastic syndrome was depicted in a female patient who underwent excision of a right parietal high grade glioma. Extensive bilateral edema of all muscle groups was reported; particularly lower limb edema extending down to the sole of the foot (Fig. 2b). We agree with O'Connell et al.

Fig. 2. WB-MRI, STIR sequence for two cases of polymyositis. (a) Case 1: idiopathic inflammatory myositis in a 27-year-old man showing mild bilateral symmetrical edema of the back (erector spinae), shoulder, and pelvic girdle muscles. Interstitial edema is seen in the subcutaneous fat of the gluteal region and thighs. Case 2: (b) polymyositis with para-neoplastic syndrome in a 44-year-old woman with a history of recurrent excised high grade glioma showing marked bilateral symmetrical edema of the shoulder girdle, pelvic girdle, and lower limb muscles down to the sole of the foot. Facial edema is seen in the posterior aspect of the right calf region, medial aspect of the left thigh, and distal left leg. Note: tumor recurrence and meningio-encephalocele are seen at the site of right parietal craniectomy.

(3) who strongly recommend screening tests for elderly patents presenting with bilateral proximal myopathy. Moreover, we stress the need of WB-MRI for metastatic work-up and exclusion of myositis with paraneoplastic syndrome in patients with malignant neoplasms presenting with suspicious clinical symptoms.

Up to one-third of the cases with polymyositis can be associated with an underlying collagen disease (22). We conducted WB-MRI for four cases with SLE and one with scleroderma. The presence of edema in overlap myositis is explained by increased amount of fluid and inflammatory infiltrate (23).

Besides inflammatory myopathy, MRI is highly efficient in the detection and discrimination of steroid induced myopathy in patients with longstanding collagen disease (24) owing to the ability to detect diffuse fatty infiltration and muscle atrophy. Moreover, MRI is the modality of choice for early detection of avascular necrosis (AVN), providing a better chance for early treatment and prevention of bone collapse (25). AVN and gluteal muscle atrophy were detected in 2/4 cases in our study (Fig. 3g).

In the literature, overlap myositis with scleroderma presents a broad spectrum of heterogeneous muscle disorders (26). A study by Zivkovic et al. (27) presented a review of case reports of localized scleroderma and described the disease as a rare idiopathic localized disorder which comprises myositis, localized fasciitis, and thickening of the overlying subcutaneous fat. Meanwhile, another study by Schanz et al. (28)

Fig. 3. Three cases of overlap myositis with SLE. (a) Case 1: marked bilateral symmetrical edema of all scanned muscles associated with fascial and interstitial edema of the overlying subcutaneous fat. Case 2: bilateral symmetrical patchy edema affecting the thigh muscles in the coronal image (b) as well as intermuscular fascial edema seen in both axial images (c, d). Case 3: mild edema in the region of the pelvic and thigh muscles (e, f). Serpiginous subarticular avascular necrosis seen in both femoral heads with interstitial reticular edema of the subcutaneous fat and streaks of fatty infiltration within the gluteus maximus muscles better depicted on T1 images (g, h).

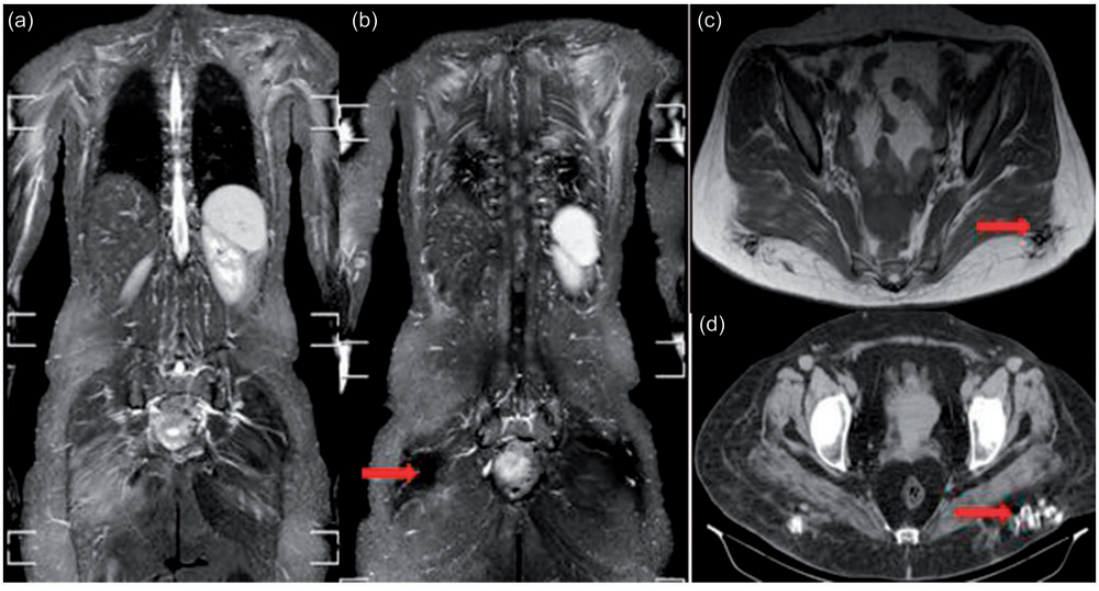

Fig. 4. Overlap myositis with scleroderma in a 39-year-old woman. Bilateral symmetrical edema of the shoulder girdle and gluteal region (a), subscapularis, latissmus dorsi, and erector spinae muscles (b). Bilateral signal void foci are seen in the posterior gluteal subcutaneous fat on both coronal STIR (b) and axial T1 (c) images. They appear as hyperdense foci of calcification on the CT scan (d).

reported bilateral symmetrical generalized myositis in 14/18 (78%) of cases recruited in their study. In our study, one case with scleroderma demonstrated bilateral symmetrical proximal upper and lower limb edema with overlying fascial and subcutaneous edema and gluteal calcification (Fig. 4).

The potential value of diffusion-weighted imaging in muscle diseases is still under investigation. It is suggested that it can increase the diagnostic sensitivity and contribute to a better understanding of the pathophysiology of striated muscle diseases. Normal muscle apparent diffusion coefficient (ADC) value is significantly higher than that of the subcutaneous fat. In cases of inflammatory myositis, cytotoxic edema results in increased ADC value (18). Diffusion tensor tractography is also a promising reliable modality to evaluate muscle shape and the orientation of muscle fibers. ADC and fractional anisotropy (FA) are reliable parameters (29).

The role of contrast-enhanced MRI techniques is still unclear. Trials to evaluate the role of gadolinium (Gd)-based contrast-enhanced MRI were published in hereditary muscular dystrophies. Yet, the role of contrast-enhanced MRI in the improvement of MR diagnostic capability is still unclear (30). More specific contrast agents such as small iron oxide particles (SPIO) may contribute to a better understanding of inflammatory and degenerative muscle diseases (9).

In conclusion, WB-MRI is the diagnostic modality of choice for cases of bilateral diffuse inflammatory myositis. It establishes early diagnosis of asymptomatic myositis, accurately detects the most severely affected muscles candidate for biopsy, and provides a reliable baseline study for the follow-up of disease progression as well as response to treatment.

Declaration of conflicting interests

The author(s) declared no potential conflicts of interest with respect to the research, authorship, and/or publication of this article.

Funding

The author(s) received no financial support for the research, authorship, and/or publication of this article.

References

1. Gupta SJ. The idiopathic inflammatory myopathies: Current perspectives and management. J Indian Rheumatol Assoc 2004;12:58–59.
2. Wedderburn LR, Rider LG. Juvenile dermatomyositis: new developments in pathogenesis, assessment and treatment. Best Pract Res Clin Rheumatol 2009;23:665–678.
3. O'Connell MJ, Powell T, Brennan D, et al. Whole-body MR imaging in the diagnosis of polymyositis. Am J Roentgenol 2002;179:967–971.
4. Karpati G, O'Ferrall EK. Sporadic inclusion body myositis: pathogenic considerations. Ann Neurol 2009;65: 7–11.
5. Dalakas MC, Hohlfeld R. Polymyositis and dermatomyositis. Lancet 2003;362:971–982.
6. Yosipovitch G, Beniamino O, Rousso I, et al. STIR magnetic resonance imaging: a non-invasive method for detection and follow-up of dermatomyositis. Arch Dermatol 1999;135:721–723.
7. Park JH, Olsen NJ. Utility of magnetic resonance imaging in the evaluation of patients with inflammatory myopathies. Curr Rheumatol Rep 2001;3:334–345.
8. Wedderburn LR, Li CK. Pediatric idiopathic inflammatory muscle disease. Best Pract Res Clin Rheumatol 2004; 18:345–358.
9. Wattjes MP, Kley RA, Fischer D. Neuromuscular imaging in inherited muscle diseases. Eur Radiol 2010;20: 2447–2460.
10. Tomasova Studynkova J, Charvat F, Jarosova K, et al. The role of MRI in the assessment of polymyositis and dermatomyositis. Rheumatology (Oxford) 2007;46: 1174–1179.
11. Quijano-Roy S, Smirnow DA, Carlier RY. Whole body muscle MRI protocol: Pattern recognition in early onset NM disorders. Neuromuscul Disord 2012;22:68–84.
12. Bohan A, Peter JB. Polymyositis and dermatomyositis. N Engl J Med 1975;292:344–347.
13. Hay EM, Bacon PA, Gordon C, et al. The BILAG index: a reliable and valid instrument for measuring clinical disease activity in systemic lupus erythematosus. QJ Med 1993;86:447–458.
14. Whiting-O'Keefe QE, Stone JH, Hellmann DB. Validity of a vasculitis activity index for systemic necrotizing vasculitis. Arthritis Rheum 1999;42:2365–2371.
15. Rider LG, Koziol D, Giannini EH, et al. Validation of manual muscle testing and a subset of eight muscles for adult and juvenile idiopathic inflammatory myopathies. Arthritis Care Res 2010;62:465–472.
16. May DA, Disler GD, Jones EA, et al. Abnormal signal intensity in skeletal muscle at MR imaging: patterns, pearls and pitfalls. Radiographics 2000;20(Suppl. 1): S295–S315.
17. Degardin A, Morillon D, Lacour A, et al. Morphologic imaging in muscular dystrophies and inflammatory myopathies. Skeletal Radiol 2010;39:1219–1227.
18. Kim HK, Lindquist DM, Serai SD, et al. Magnetic resonance imaging of pediatric muscular disorders recent advances and clinical applications. Radiol Clin N Am 2013;51:721–742.
19. Cantwell C, Ryan M, O'Connell M, et al. A comparison of inflammatory myopathies at whole-body turbo STIR MRI. Clin Radiol 2005;60:261–267.
20. Ladd PE, Emery KH, Salisbury SR, et al. Juvenile dermatomyositis: correlation of MRI at presentation with clinical outcome. Am J Roentgenol 2011;197:W153–W158.
21. Miles L, Bove KE, Lovell D, et al. Predictability of the clinical course of juvenile dermatomyositis based on initial muscle biopsy: a retrospective study of 72 patients. Arthritis Rheum 2007;57:1183–1191.

22. Tandan R. Dermatomyositis and polymyositis. In: Braunwald E, Fauci AS, Kasper DL, et al., eds. Harrison's Principles of Internal Medicine, 15th ed. New York, NY: McGraw-Hill, 2001:1896–1901.
23. Ribeiro D, Neto C, Almeida F, et al. Imaging findings of musculoskeletal disorders associated with systemic lupus erythematosus. Radiol Bras 2011;44:52–58.
24. Dion E, Cherin P, Payan C, et al. Magnetic resonance imaging criteria for distinguishing between inclusion body myositis and polymyositis. J Rheumatol 2002;29: 1897–1906.
25. Öner AY, Aggunlu L, Akpek S, et al. Staging of hip avascular necrosis: is there a need for DWI? Acta Radiol 2011;52:111–114.
26. Paik JJ, Mammen A, Wigley FM, et al. Myopathy in scleroderma, its identification, prevalence, and treatment: lessons learned from cohort studies. Curr Opin Rheumatol 2014;26:124–130.
27. Zivkovic SA, Freiberg W, Lacomis D, et al. Localized scleroderma and regional inflammatory myopathy. Neuromuscul Disord 2014;24:425–430.
28. Schanz S, Henes J, Ulmer A, et al. Magnetic resonance imaging findings in patients with systemic scleroderma and musculoskeletal symptoms. Eur Radiol 2013;23: 212–221.
29. Kermarrec E, Budzik JF, Khalil C, et al. In vivo diffusion tensor imaging and tractography of human thigh muscles in healthy subjects. Am J Roentgenol 2010;195: W352–W356.
30. Schmidt S, Vieweger A, Obst M, et al. Dysferlin-deficient muscular dystrophy: gadfluorine M suitability at MR imaging in a mouse model. Radiology 2009;250:87–94.